



1
2 DR BENJAMIN LUKE TURNER (Orcid ID : 0000-0002-6585-0722)

3
4
5 Article type : Research Article

6 Editor : Cynthia Chang

7
8
9 **Contrasting patterns of plant and microbial diversity during long-term**
10 **ecosystem development**

11
12 **Benjamin L. Turner^{1,2}, Graham Zemunik^{1,2}, Etienne Laliberté^{3,2}, Jeremy J. Drake⁴, Frank A. Jones^{1,5},**
13 **Kristin Saltonstall¹**

14
15 ¹ *Smithsonian Tropical Research Institute, Apartado 0843-03092, Balboa, Ancon, Republic of Panama*

16 ² *School of Biological Sciences, The University of Western Australia, 35 Stirling Highway, Perth, WA 6009,*
17 *Australia*

18 ³ *Institut de recherche en biologie végétale, Département de sciences biologiques, Université de*
19 *Montréal, 4101 Sherbrooke Est, Montréal H1X 2B2, Canada*

20 ⁴ *Smithsonian Astrophysical Observatory, 60 Garden Street, Cambridge, MA 02138, USA*

21 ⁵ *Department of Botany and Plant Pathology, Oregon State University, Corvallis, OR 97331, USA*

22 Correspondance: Email TurnerBL@si.edu

23
24 **Abstract**

25 **1.** Long-term ecosystem development involves changes in plant community composition and diversity
26 associated with pedogenesis and nutrient availability, but comparable changes in soil microbial
27 communities remain poorly understood. In particular, it is unclear whether the diversity of plants and
28 microbes respond to similar abiotic drivers, or become decoupled as resources change over long time
29 scales.

This is the author manuscript accepted for publication and has undergone full peer review but has not been through the copyediting, typesetting, pagination and proofreading process, which may lead to differences between this version and the Version of Record. Please cite this article as doi: 10.1111/1365-2745.13127

This article is protected by copyright. All rights reserved

30 **2.** We characterised communities of archaea, bacteria, and fungi in soils along a 2-million-year
31 chronosequence of coastal dunes in a biodiversity hotspot in Western Australia. The chronosequence
32 involves marked changes in soil pH and nutrient availability that drive major shifts in plant community
33 composition and diversity as soils age.

34 **3.** Patterns of α -diversity for microbial groups differed along the chronosequence. Bacterial α -diversity
35 was greatest in intermediate-aged soils, archaeal diversity was greater in young alkaline or
36 intermediate-aged soils, while fungal α -diversity – like plant diversity – was greatest in old, strongly
37 weathered soils where phosphorus is the limiting nutrient.

38 **4.** Changes in microbial community composition along the chronosequence were explained primarily by
39 the long-term decline in soil pH, with a smaller influence of the relative abundance of plant nutrient-
40 acquisition strategies. However, changes between the prokaryote and fungal communities, and between
41 fungal and plant communities, became increasingly decoupled along the chronosequence,
42 demonstrating that the coordination of change in biological communities by abiotic drivers becomes
43 weaker during long-term ecosystem development.

44 **5.** Several bacterial taxa, including DA101 (Verrucomicrobia), "*Candidatus Solibacter*" (Acidobacteria)
45 and *Gaiella* (Actinobacteria), were particularly abundant on the oldest dunes, indicating that they are
46 adapted to acquire phosphorus from extremely infertile soils. However, we cannot disentangle the
47 influence of phosphorus from the long-term decline in soil pH along the chronosequence.

48 **6. Synthesis:** These results provide evidence for contrasting patterns of plant and microbial community
49 composition and α -diversity in response to acidification and nutrient depletion during long-term
50 pedogenesis.

51 52 **1. INTRODUCTION**

53 Soils harbour a remarkable diversity of microbes and there is currently considerable interest in
54 understanding how environmental properties influence biogeographical patterns below ground. For
55 example, recent studies have described the distributions of bacterial, archaeal, and fungal taxa in soils
56 worldwide (Tedersoo et al., 2014; Thompson et al., 2017; Delgado-Baquerizo et al., 2018), and there is
57 evidence that microbial community composition varies predictably in relation to environmental
58 parameters such as temperature (Zhou et al., 2016), soil pH (Lauber et al., 2009; Rousk et al., 2010) and
59 fertility (Leff et al., 2015). Of these, soil pH is a particularly important constraint on bacterial diversity,
60 leading to lower diversity in both strongly alkaline (pH > 7.5) and acidic (pH < 5) soils (Fierer, 2017).
61 However, patterns of below ground microbial diversity do not respond consistently to the abiotic

62 environment (Hendershot et al., 2017), indicating that much remains to be learned about drivers of
63 below ground diversity.

64
65 A central question is the extent to which soil microbial diversity is related to plant diversity. The strong
66 functional relationships between above and below ground communities suggest that they should be
67 correlated positively (Kardol & Wardle, 2010). Yet the α -diversity of bacteria, fungi, and archaea appear
68 unrelated to plant diversity in grassland ecosystems (Prober et al., 2015), while a study of old-field
69 succession found that plant community change was associated only with the fungal community, because
70 bacterial community change was determined primarily by abiotic conditions, particularly soil pH (Cline &
71 Zak, 2015). The relationship between plant and fungal α -diversity holds worldwide (Tedersoo et al.,
72 2014) and presumably reflects symbiotic relationships (i.e. mycorrhizal fungi) and the direct dependence
73 of fungi on inputs of plant detritus. We might therefore expect links between above and below ground
74 communities to differ for bacteria and fungi in response to variation in abiotic properties during long-
75 term ecosystem development.

76
77 Soil chronosequences offer an important opportunity to assess the influence of soil properties on
78 biological diversity. A chronosequence is a series of soils that differ only in the time since the onset of
79 soil formation, with other soil-forming factors (climate, topography, parent material, organisms)
80 remaining relatively constant (Stevens & Walker, 1970). This allows patterns of soil and ecosystem
81 development to be studied using a space-for-time approach (Walker et al., 2010). Long-term
82 pedogenesis involves the gradual acidification of soil and leads to predictable changes in nutrient
83 availability, with a shift from nitrogen limitation on young soils to phosphorus limitation on old soils
84 (Vitousek & Farrington, 1997; Laliberté et al., 2012; Coomes et al., 2013). This shift drives parallel
85 changes in the biomass (Wardle, Walker & Bardgett, 2004) and diversity (Laliberté et al., 2013; Laliberté,
86 Zemunik & Turner, 2014) of associated plant communities. Below ground responses to long-term
87 ecosystem development have been less frequently studied, but bacterial and fungal communities have
88 been shown to change rapidly during the progressive (Cutler, Chaput & van der Gast, 2014; Castle et al.,
89 2016; Roy-Bolduc et al., 2016) and retrogressive (Tarlera et al., 2008; Jangid et al., 2013; Uroz et al.,
90 2014) stages of ecosystem development. In particular, several studies have examined below ground
91 communities along the Franz Josef post-glacial chronosequence, finding differences related to declining
92 soil pH and phosphorus availability that are most strongly linked to plant community change during the

93 early progressive stage (Williamson, Wardle & Yeates, 2005; Allison et al., 2007; Jangid et al., 2013;
94 Turner et al., 2017).

95
96 The Jurien Bay chronosequence in Western Australia provides an opportunity to examine patterns of
97 plant and soil microbial diversity during long-term ecosystem development. The chronosequence is
98 formed of coastal dunes deposited during interglacial marine high-stands since the Early Pleistocene,
99 approximately two-million years ago (Wyrwoll, Turner & Findlater, 2014; Turner & Laliberté, 2015).
100 Nutrient limitation of plant productivity shifts from nitrogen on young soils to phosphorus on old soils
101 (Laliberté et al., 2012), reflected in a marked increase in the diversity of nutrient acquisition strategies in
102 the plant community as soils age (Zemunik et al., 2015). The chronosequence occurs in a global
103 biodiversity hotspot, and plant diversity increases continually throughout the sequence, driven by
104 environmental filtering from the regional species pool as pH declines during long-term pedogenesis
105 (Laliberté, Zemunik & Turner, 2014). Recent studies have characterised changes in the composition and
106 diversity of specific symbiotic microbial groups along the sequence (Krüger et al., 2015; Albornoz et al.,
107 2016; Birnbaum et al., 2018), but there is so far little information on comparable changes in the broader
108 soil microbial community, including non-symbiotic microbes, although there is a shift from bacterial to
109 fungal energy channels in the below ground food web as soils age (Laliberté et al., 2017). Here, we
110 studied bacterial, archaeal, and fungal communities along the Jurien Bay chronosequence. We aimed to
111 quantify overall patterns of soil microbial diversity along the chronosequence and assess the extent to
112 which the diversity of above and below ground communities are coordinated during long-term
113 ecosystem development.

114

115 **2. MATERIALS AND METHODS**

116 **2.1 The Jurien Bay Chronosequence**

117 The two-million-year Jurien Bay chronosequence is located in Western Australia, approximately 200 km
118 north of Perth (30°01'–30°24' S, 114°57'–115°11' E). The climate is Mediterranean, with hot, dry
119 summers and cool, moist winters. The mean annual temperature at Jurien Bay is 19°C. Mean annual
120 rainfall is 533 mm, with a six month dry season between October and April. The chronosequence has
121 been described in detail elsewhere, including the soils (Turner & Laliberté, 2015; Turner, Hayes &
122 Laliberté, 2018) and plant communities (Laliberté et al., 2012; Laliberté, Zemunik & Turner, 2014;
123 Zemunik et al., 2015; 2016). The chronosequence is formed of coastal sand deposits formed by
124 Quaternary sea level fluctuations and three main dune systems are recognized, representing dunes

125 formed during the Holocene (Quindalup dunes), Middle Pleistocene (Spearwood dunes), and Early
126 Pleistocene, or possible late Pliocene (Bassendean dunes) (Kendrick, Wyrwoll & Szabo, 1991; Laliberté et
127 al., 2012; Wyrwoll, Turner & Findlater, 2014). Detailed maps of the plots, dune formations, and
128 associated soils can be found elsewhere (Turner & Laliberté, 2015; Zemunik et al., 2016).

129
130 Soils show a clear pattern of pedogenesis along the chronosequence and have been studied in detail
131 (Turner & Laliberté, 2015; Turner, Hayes & Laliberté, 2018). Holocene soils are formed of calcareous
132 sand and are initially strongly alkaline. As the soil acidifies, carbonate is dissolved and leached from the
133 profile, leaving residual quartz sand over a petrocalcic horizon, with iron oxide coatings giving the sand a
134 characteristic yellow colour. As pedogenesis proceeds, iron oxides are leached from the soil by
135 podzolisation, yielding bleached quartz sand many meters deep on the oldest dunes.

136
137 Soil development is accompanied by marked changes in nutrient availability. Young soils are relatively
138 high in phosphorus but contain little nitrogen. As pedogenesis proceeds, nitrogen accumulates rapidly
139 (i.e. in hundreds to thousands of years) and then declines, while phosphorus declines continuously, so
140 that old soils contain extremely low phosphorus concentrations, among the lowest reported worldwide
141 (Turner & Laliberté, 2015). Plant productivity therefore appears limited by nitrogen on young soils and
142 by phosphorus on old soils (Laliberté et al., 2012), reflected in marked shifts in foliar nutrients (Hayes et
143 al., 2014) and plant nutrient acquisition strategies (Zemunik et al., 2015) along the chronosequence.

144
145 The chronosequence is located in a global biodiversity hotspot known as the Southwest Australian
146 Floristic Region (Myers et al., 2000). The vegetation is Mediterranean low shrubland known as kwongan
147 (Hopper, 2014), dominated by sclerophyllous shrubs and trees with remarkably high species richness
148 and endemism (Lamont, Hopkins & Hnatiuk, 1984). Along the chronosequence, families such as
149 Fabaceae and Myrtaceae are common on younger dune systems, while Proteaceae become more
150 common on older dunes (Zemunik et al., 2016). There is a marked increase in plant species richness with
151 soil age along the chronosequence (Laliberté, Zemunik & Turner, 2014), a pattern consistent with other
152 long-term retrogressive chronosequences worldwide (Laliberté et al., 2013).

153 154 **2.2 Soil and plant sampling**

155 Soil samples were collected from five replicate 10 × 10 m plots on each of five stages of the
156 chronosequence spanning approximately 2 million years of ecosystem development. In each plot,

157 samples were taken from five points from the upper 20 cm of the soil using a 5 cm diameter sand auger,
158 and combined into a single composite sample per plot. For microbial community analysis, soils were
159 stored on ice and then frozen within 6 h. Subsamples for physical and chemical analysis were air-dried
160 for 7 d at ambient room temperature.

161

162 The plant communities along the chronosequence have been studied in detail (Laliberté, Zemunik &
163 Turner, 2014; Zemunik et al. 2015; Zemunik et al. 2016). Briefly, all vascular plants rooted in each 10 ×
164 10 m plot were recorded and identified to the species level. Canopy cover and number of individuals for
165 each plant species was estimated in seven randomly-located 2 m × 2 m subplots within each 10 m × 10
166 m plot. The full data set and detailed methodology is available online (doi:
167 10.4227/05/56AEB32FC11D4).

168

169 **2.3 Soil analysis**

170 Soil analysis was described previously (Laliberté et al., 2012; Turner & Laliberté, 2015; Turner, Hayes &
171 Laliberté, 2018), although we performed new analyses using the same methods on the samples taken
172 for this study. Briefly, soil pH was determined in both deionized water and 10 mm CaCl₂ in a 1:2 soil to
173 solution ratio. Total carbon and nitrogen were determined simultaneously by automated combustion
174 and gas chromatography using a Thermo Flash 1112 elemental analyser (CE Elantech, Lakewood, NJ,
175 USA). Total phosphorus was determined by ignition (550°C, 1 h) and extraction in 1 M H₂SO₄ (16 hours,
176 1:50 soil to solution ratio) (Walker & Adams, 1958). Exchangeable cations were determined by
177 extraction in 0.1 M BaCl₂ (2 h, 1:30 soil to solution ratio) and detection by inductively-coupled plasma
178 optical-emission spectrometry (ICP–OES) with an Optima 7300 DV (Perkin-Elmer Ltd, Shelton, CT, USA)
179 (Hendershot, Lalande & Duquette, 2008). Carbonate was determined by mass loss after acidification
180 (Loeppert & Inskeep, 1996) and organic C was calculated as the difference between total C and CaCO₃-C.
181 Readily-exchangeable phosphate (resin phosphorus) was determined by extraction with anion exchange
182 membranes (Turner & Romero, 2009). Total exchangeable bases (TEB) was calculated as the sum of the
183 charge equivalents of Ca, K, Mg and Na; effective cation exchange capacity (ECEC) was calculated as the
184 sum of the charge equivalents of Al, Ca, Fe, K, Mg, Mn and Na; base saturation was calculated by (TEB /
185 ECEC) × 100.

186

187 **2.4 DNA extraction and sequencing**

188 We used the MoBio Laboratories PowerMax Soil DNA extraction kit to maximize DNA recovery from
189 these sandy soils. Soil (10 g fresh weight) was extracted following the manufacturer's instructions. The
190 final solutions containing DNA were frozen, lyophilized, and stored at -80°C until they were
191 resuspended in 2 mL Tris-EDTA buffer prior to sequencing. Two samples did not amplify well (one
192 sample from each of the two Holocene dunes) and were omitted from further analysis.

193
194 Microbial diversity was assessed using high throughput sequencing to characterize the distribution and
195 abundance of soil archaea, bacteria and fungi. For bacteria and archaea we used the V4 hypervariable
196 region of the 16S RNA gene using the 515F–806R primer pair (Caporaso et al., 2011). For fungi, we
197 sequenced the first internal transcribed spacer (ITS1) region of the rRNA operon, using the primer pair
198 ITS1F and ITS2R (White et al., 1990). The primers included all necessary Illumina adapters with barcodes
199 to distinguish samples. The bacterial 806R primer included a 10 bp barcode sequence, while the ITS1F
200 and ITS2R primers each included an 8 bp barcode sequence, allowing us to multiplex multiple samples.
201 PCR reactions were done in triplicate 25 μL reactions with 5Prime 2X Hot Mastermix. Triplicates were
202 pooled and cleaned by excising the amplified bands from a gel and purifying with the QIAQuick Gel
203 Extraction kit (Qiagen). Samples were then concentrated by ethanol precipitation and quantified on a
204 Qubit. Equal quantities of each sample were then pooled together and the resulting libraries (one 16S,
205 one ITS) concentrated with ethanol precipitation. Final library concentrations were estimated using both
206 a BioAnalyzer and qPCR. Libraries were sequenced on paired end 2x250 bp Illumina Miseq runs at the
207 STRI Ecological and Evolutionary Genomics Laboratory.

208

209 **2.5 Bioinformatics**

210 Sequence data were analyzed using QIIME 1.9.1 (Caporaso et al., 2010a; Caporaso et al., 2010b),
211 primarily using default parameter values. Sequences were initially filtered for $q > 20$ during the split-
212 libraries step. Chimera checking was done using usearch_61 (Edgar, 2010). We used the Greengenes
213 13_8 (McDonald et al., 2012) and the Unite databases (January 2016 release; Abarenkov et al., 2010) to
214 assign taxonomy for 16S and ITS rRNA sequences respectively. Raw sequences were mapped to
215 phylotypes at the 97% similarity threshold using the 'usearch' classifier. For fungi, we used the 'dynamic'
216 similarity threshold and the BLAST method (Altschul et al., 1990) for assigning taxonomy; all unidentified
217 OTUs and those corresponding to the Kingdom Protista were removed prior to downstream analysis
218 (<4% of total OTUs). Representative sequences, phylotype abundance tables, and corresponding sample
219 information is available online (doi: 10.6084/m9.figshare.7180388).

220

221 **2.6 Statistical analyses**

222 **2.6.1 Alpha diversity**

223 Rarefaction is well suited for comparing richness among samples (Magurran, 2004), because it samples a
224 fixed number of sequences for all samples and therefore controls for differences in sequencing depth.

225 We therefore used rarefied richness as our primary measures of α -diversity of both plant and microbial
226 communities. We also calculated Simpson's $1/D$ and the Shannon diversity metric, both commonly used
227 for plant communities, although the Shannon metric is least useful for microbial communities because it
228 relies on the assumption that the community has been completely sampled, which is untrue below
229 ground. Finally, we calculated diversity in microbial communities using the Chao-1 estimator, which
230 attempts to account for the many unmeasured rare species that occur belowground (Chao, 1984).

231

232 All statistical analyses were done in R (version 3.3.1). The Shannon's and inverse ($1/D$) Simpson's
233 diversity indices were calculated for the microbial communities using the 'diversity' function from
234 'vegan'. Richness was estimated with the non-parametric 'chao' estimator and OTU accumulation curves
235 of the mean richness for all stages were calculated from 100 permutations using the 'estaccumR'
236 function from 'vegan'. Richness per plot was rarefied to the minimum number of sequences across all
237 plots of the chronosequence and was calculated with the 'rarefy' vegan function. Differences between
238 stages were assessed by Tukey's Honest Significant Differences tests.

239

240 **2.6.2 NMDS ordinations**

241 To investigate relationships between soil properties and biological communities, data for each
242 taxonomic group were ordinated by NMDS using the 'metaMDS' function from 'vegan', with the data
243 standardised by the modified Gower distance (Anderson et al., 2006) and logarithmic bases set to 2.
244 Higher bases give less weight to changes in abundance vs. changes in composition: a base 10 puts the
245 same weight for a change in abundance from 10 to 100 as a change in composition from 0 to 1
246 (Anderson et al. 2006). For microbial communities, dissimilarities were calculated using the lowest
247 taxonomic level (i.e. OTU) using the 'vegdist' function from vegan. Stress values represent a measure of
248 the distortion in the multi-dimensional scaling, with lower stress indicating a better two-dimensional
249 representation.

250

251 **2.6.3 Redundancy analysis**

252 To assess the influence of soil properties or nutrient acquisition strategies on biological communities we
253 performed a redundancy analysis (RDA) using the 'rda' function from 'vegan', with the response being
254 either the Hellinger-transformed community (ITS or 16S) data or dissimilarities calculated with 'vegdist'
255 after standardization with the modified Gower distance ('logbase' set to 2 or 10). When the modified
256 Gower distance was used, the 'capscale' function was used to perform the redundancy analysis instead
257 of 'rda'. The threshold for the forward selection (adjR2thresh parameter) was the adjusted R^2 from an
258 RDA run with the full set of soil variables (pH CaCl_2 , total carbon, total nitrogen, total phosphorus,
259 organic carbon, carbonate, resin phosphorus, Al, Ca, Fe, K, Mg, Mn, Na, ECEC). Significance of the model
260 was assessed with the 'permutest' function. Hellinger-transformation and standardization by the
261 modified Gower distance of the ordination data was done using the 'decostand' function from vegan.
262 The constraining variables for the analysis, soil and nutrient-acquisition strategies, were combined and
263 the set was then reduced to a minimal explanatory set by forward and backward selection using
264 'ordistep' from vegan. Because there were many nutrient-acquisition strategies, some with several
265 strategies in combination, the set of nutrient-acquisition strategies used in the selection process
266 combined these strategies into larger strategy classes, following Zemunik et al. (2015): arbuscular
267 mycorrhizal (but not ectomycorrhizal), ectomycorrhizal (and possibly others), nitrogen-fixing (and
268 possibly others), ericoid mycorrhizal, parasites (and possibly others), other mycorrhizal, non-mycorrhizal
269 (all types).

270

271 **2.6.4 Procrustes ANOVA and regressions**

272 To compare patterns of change among the 16S (bacteria and archaea), ITS, and vegetation communities
273 we performed Procrustes analyses on the NMDS ordinations. We used the 'procrustes' function from
274 the vegan R package and determined the significance of the transformations with the 'protest' function.
275 To assess whether differences existed between pairwise combinations of the fungal, 16S and vegetation
276 community data across the different sampling regions, we used the Procrustean association metric
277 (PAM) with an analysis of variance (ANOVA) (Lisboa et al., 2014). In essence, this analysis can help detect
278 differences among groups of sites by using the residuals from the Procrustes rotation, so that pairs of
279 points that are further apart have greater residuals and the ordinations are therefore considered less
280 similar or more decoupled. Because Procrustes rotations require the same dimensionality of the two
281 input matrices, and because it is important to have a minimal quantified amount of the variation
282 explained in the source ordinations, the community data sets were first Hellinger-transformed and then
283 ordinated by principal component analysis (PCA). A minimum number of principal components (PCs) to

284 represent at least 70% of the variation were used from each PCA ordination to form matrices of the
285 same dimension for each community data set.

286

287 The residuals from the Procrustes rotation were then used as the response of a linear regression with
288 the chronosequence stages as the predictor variable. Because the residuals of the regression using the
289 'lm' function exhibited heteroscedasticity, the 'gls' function from 'nlme' was used with a variance
290 function (varExp) to achieve constant variance of the model residuals. Confidence intervals from the
291 model fit were calculated with the 'effect' function from the 'effects' package.

292

293 **2.6.5 Community differences due to soil or vegetation**

294 The PAM was combined with PCA ordination, in a manner outlined by Lisboa et al. (2014), to detect
295 community differences due to either soil or the associated vegetation. Similar to the ANOVA using the
296 PAM, the community data sets were Hellinger-transformed and ordinated by PCA. The soil and
297 (Hellinger-transformed) vegetation data sets were also ordinated by PCA. From these ordinations, the
298 PC scores (from a minimum subset of all PCs, chosen to explain at least 70% of the variation) were used
299 in Procrustes rotation, with the fungal and 16S communities being compared against the soil and
300 vegetation (four comparisons in total). The residuals from these Procrustes rotations were then
301 assembled into a matrix (sites as columns and rows containing the residuals from each Procrustes
302 rotation) and the matrix was then ordinated by PCA. This technique allows for visual assessment of
303 differences produced by either the soil or vegetation, although no statistical significance can be ascribed
304 due to the limited sample size (4) of the ordination.

305

306 **2.6.6 Multivariate regression trees**

307 We used multiple regression trees to further investigate the influence of soil properties or nutrient
308 acquisition strategies on variation in the 16S and ITS communities, which allow prediction of site
309 groupings based on binary decisions. The combined set of soil and nutrient-acquisition strategies
310 (determined as described above) was used as the predictor in the 'mvpart' function from the 'mvpart'
311 package. The response was the Hellinger-transformed 16S (bacteria and archaea) or fungal community
312 data. The 'ggdendro' package was used to produce the binary trees with each branch length
313 corresponding to the amount of variation explained.

314

315 **3. RESULTS**

3.1 Soil properties

Soils were alkaline (pH 8.6) on Holocene dunes and slightly to moderately acidic on Middle Pleistocene (pH 6.4) and Early Pleistocene (pH 6.0) dunes (Table 1). Holocene soils contained carbonate, but this was absent from Pleistocene dunes (the carbonate is dissolved and leached from the profile as soils acidify during pedogenesis). Concentrations of organic carbon, nitrogen, phosphorus, and cations declined throughout the sequence. In particular, resin phosphorus declined from $4.38 \pm 2.52 \text{ mg P kg}^{-1}$ on the youngest Holocene dunes to $< 1 \text{ mg P kg}^{-1}$ on Pleistocene dunes, while total phosphorus declined from $429 \pm 38 \text{ mg P kg}^{-1}$ on the youngest Holocene dunes to $5.2 \pm 1.2 \text{ mg P kg}^{-1}$ on the oldest Pleistocene dunes (Table 1), thus representing some of the lowest phosphorus soils globally. Soils at all stages were sands ($> 95\%$ sand) with high base saturation ($\geq 99\%$).

3.2 Microbial community composition

We obtained almost 5 million sequences for 16S and more than 1.5 million sequences for ITS. Mean numbers of sequences, total OTUs, and observed OTUs for each dune system are shown in Table 2. OTU accumulation curves for 16S and ITS communities are shown in Supplementary Fig. 1.

The 16S community (i.e., bacteria and archaea) was dominated by Actinobacteria (24.7–28.9%), Proteobacteria (29.3–33.5%), and Acidobacteria (10.4–15.4%) across all sites, with smaller proportions of Bacteroidetes (4.0–6.2%), Chloroflexi (1.9–3.1%), Gemmatimonadetes (1.3–5.8%), Planctomycetes (5.3–6.9%), and Verrucomicrobia (3.1–7.0%) (Table 3). Other individual phyla accounted for 1% or fewer of the total OTUs. Archaea constituted 0.4–3.9% of total abundance, predominantly in the ammonia-oxidizing genus *Nitrososphaera* (phylum Crenarchaeota).

The fungal community included a considerable proportion of unidentified fungi (21.6–56.4%). Of the identified phyla, the majority were Ascomycota (26.7–54.8%) and Basidiomycota (9.5–22.8%), with Chytridiomycota, Glomeromycota, Rozellomycota, and Zygomycota each accounting for $\leq 3.0\%$ (Table 3).

Microbial taxa showed contrasting patterns during ecosystem development (Fig. 1, Table 3). Of the dominant bacterial taxa, the abundance of Acidobacteria, Alphaproteobacteria, Planctomycetes, and Verrucomicrobia increased significantly along the chronosequence (Kruskal-Wallis, $FDR-p < 0.05$), while the Archaea, Chloroflexi, Deltaproteobacteria, Gammaproteobacteria and Gemmatimonadetes all

348 declined (Table 3). However, there was considerable variation among classes within a phylum, and
349 among orders within a class (e.g. for the Proteobacteria; Fig. 1). For fungi, Ascomycota and
350 Basidiomycota increased in abundance along the sequence, while all other phyla declined (Table 3).

351
352 A number of bacterial genera were abundant throughout the chronosequence, including *Rhodoplanes* (a
353 phototrophic Alphaproteobacteria in the order Rhizobiales), *Mycobacterium* (Actinobacteria), and
354 *Solirubrobacter* (the only genus in the Actinobacteria family Solirubrobactereaceae) (Kim et al., 2007).
355 Common families were the Chitinophagaceae (Bacterioidetes), Pseudonocardiaceae (Actinobacteria),
356 and the Rhodospirillaceae (purple nonsulfur photosynthetic bacteria in the Alphaproteobacteria), the
357 latter being particularly abundant on the oldest soil.

358
359 Soil pH and resin phosphorus were correlated strongly in our dataset, so it is difficult to isolate the
360 influence of these variables on individual taxa (Supplementary Fig. 2). However, several bacterial taxa
361 were most abundant in the older, low phosphorus soils. In particular, the genus DA101
362 (*Verrucomicrobia*) was the most abundant single genus in the two oldest soils (Fig. 2a). Other genera
363 that were particularly abundant at low phosphorus were “*Candidatus Solibacter*” (Acidobacteria),
364 *Gaiella* (the only genus in the Actinobacteria family Gaiellaceae) (Albuquerque et al., 2011), and
365 “*Candidatus Koribacter*” (Acidobacteria) (Fig. 2a). Both “*Candidatus Koribacter*” and “*Candidatus*
366 *Solibacter*”, which are closely related, were isolated originally from Australian pasture soil (Sait,
367 Hugenholtz & Janssen, 2002). In addition, the relative abundance of a number of families increased
368 markedly on the oldest, low phosphorus soils, including Acetobacteraceae (Alphaproteobacteria),
369 Acidobacteriaceae (Acidobacteria), Caulobacteraceae (Alphaproteobacteria), and Conexibacteraceae
370 (constituting two species of Gram-positive mesophilic members of the Actinobacteria) (Fig. 2b).

371
372 The basidiomycete genera *Cortinarius* and *Sebacina* (an ecto/ericoid-mycorrhizal fungus) were the most
373 abundant fungal genera on the oldest soils. While not common (< 0.5% of total abundance), fungi from
374 the phylum Glomeromycota were more diverse and abundant in the younger soils (Fig. 3a), and the
375 OTUs that were detected tended to differ between the younger and older soils (Fig. 3b). The
376 Glomeromycota became much less variable among plots within a stage during later stages of the
377 chronosequence, despite the decreasing proportion of arbuscular mycorrhizal plants along the
378 chronosequence (Zemunik et al., 2015).

379

380 Patterns of bacterial taxa associated with symbiotic nitrogen fixation differed markedly along the
381 chronosequence. Of the families in the Proteobacteria that include a number of nitrogen-fixing genera,
382 the Bradyrhizobiaceae varied little along the chronosequence, while the Hyphomicrobiaceae and
383 Burkholderiaceae increased in abundance (Fig. 3c). Two families declined significantly on old soils
384 (Phyllobacteriaceae and Rhizobiaceae). The relative abundance of genus *Frankia* (Actinobacteria)
385 decreased significantly on older soils (Fig. 3c; FDR $p < 0.05$), while *Rhizobium* (in the
386 Alphaproteobacteria) peaked in intermediate-aged soils (not shown).

387

388 **3.3 Alpha diversity**

389 Patterns of diversity varied between microbial communities along the chronosequence (Fig. 4). Based on
390 rarefied richness, inverse Simpson, and Shannon indices, α -diversity in the fungal community was lowest
391 in young soils and increased continually along the chronosequence. In contrast, α -diversity in the
392 bacterial community followed a unimodal pattern, being initially low in the youngest soils, increasing to
393 a maximum in intermediate-aged soils, and then declining to lowest values in the oldest soils (although
394 differences were not significant for Simpson's 1/D). For archaea, α -diversity by rarefied richness
395 followed a similar pattern to bacteria, reaching a maximum in intermediate-aged soils. However, by
396 other measures (Simpson, Shannon) archaeal diversity declined continually throughout the
397 chronosequence. Diversity patterns according to the Chao-1 metric were similar to those for rarefied
398 richness, with archaeal and bacterial diversity peaking in intermediate-aged soils, and fungal diversity
399 increasing throughout the chronosequence (Table 2).

400

401 As in previous broader assessments of the plant community along the chronosequence (Zemunik et al.
402 2015; 2016), plant diversity increased continuously along the chronosequence (Fig. 4). This was clearest
403 for rarefied richness, but less so for Shannon or Simpson metrics for the subset of plots studied here. For
404 patterns at the family level, of particular note is that the relative abundance of plants forming cluster-
405 roots, predominantly in the family Proteaceae, increased markedly on the oldest dunes (Table 3).

406

407

408 **3.4 NMDS ordinations**

409 Ordination of both bacterial and fungal communities revealed a clear separation of the communities in
410 the younger Holocene soils as opposed to the older soils (Fig. 5a,b). In addition, the oldest (Early
411 Pleistocene) soils were distinct from the two Middle Pleistocene soils for both 16S and ITS. For the

412 vegetation community, there was clear separation of sites from each chronosequence stage, including
413 the youngest Middle Pleistocene soils (Fig. 5c).

414

415 **3.5 Redundancy analysis**

416 The minimal set of soil variables and nutrient acquisition strategies selected for the 16S community data
417 (Fig. 6a) explained far more of the variation than for the fungal community data (Fig. 6b). When the 16S
418 community data were Hellinger transformed, the first constrained axis of the ordination explained 49%
419 of the total variation. For the ITS community, the first constrained axis of the ordination explained only
420 18% of the total variation. For both communities, the first axis was associated primarily with soil pH and
421 total N, while the second axis reflected the abundance of plants associated with particular mycorrhizal
422 communities – arbuscular mycorrhizas for the 16S community, and ectomycorrhizas for the ITS
423 community – although the secondary axes explained only a small proportion (5%) of the total variation.

424

425 **3.6 Procrustes rotations**

426 Procrustes rotations of the NMDS ordinations revealed stronger coordination of change in biological
427 communities on the younger dunes (i.e. vector length increased for older dunes), and overall greater
428 similarity of change in 16S and ITS communities than either of the microbial communities with the
429 vegetation community (Supplementary Fig. 3). Thus, the procrustes rotation for the 16S and ITS
430 communities (logbase 10) produced a greater Procrustes correlation (i.e. greater similarity: $r = 0.959$;
431 Supplementary Fig. 3a) than the rotations of the 16S and vegetation communities ($r = 0.859$;
432 Supplementary Fig. 3b), and the fungal and vegetation communities ($r = 0.856$; Supplementary Fig. 3c).

433

434 **3.7 Procrustes ANOVA**

435 Based on the residuals from the Procrustes rotations, we found significant differences ($p < 0.05$) in
436 changes in the vegetation and ITS communities (Fig. 7a), and between the fungal and 16S communities
437 (Fig. 7b) along the chronosequence, but not between the vegetation and 16S communities (Fig. 7c). As
438 shown by the Procrustes errors (Supplementary Fig. 3), communities from the two Holocene stages
439 were better coordinated than those from all other chronosequence stages (i.e. residuals were smaller
440 on Holocene dunes; Fig. 7), demonstrating increasing decoupling between the fungal community and
441 both the bacterial and vegetation communities on the older stages.

442

443 **3.8 Multivariate regression trees**

444 Trees created with the multivariate regression methodology generally had soil variables at selection
445 nodes (Supplementary Fig. 4). The Holocene soils were always in groups by themselves, but the Middle
446 and Early Pleistocene soils were generally spread across several nodes. Total carbon occupied the first
447 order node for the fungal community (i.e. separating soils with and without carbonate), with subsequent
448 nodes formed by soil pH and exchangeable iron. For bacteria, soil pH was the first order node, with a
449 variety of soil properties occupying subsequent nodes.

450

451 **4. DISCUSSION**

452 Long-term pedogenesis leads to shifts in plant community composition and diversity, but corresponding
453 patterns below ground remain poorly understood. By studying microbial communities in soils spanning
454 two million years of pedogenesis in a global biodiversity hotspot, we find evidence for contrasting
455 patterns of diversity in archaea, bacteria, fungi, and plants during long-term ecosystem development. In
456 particular, trends in α -diversity differed along the chronosequence, peaking in young or intermediate-
457 aged soils for bacteria and archaea, but increasing continuously for fungi and plants. This general
458 pattern is consistent with a recent study showing that soil food webs shift from bacterial- to fungal-
459 dominated along the Jurien Bay sequence (Laliberté et al., 2017). We also find that although abiotic
460 properties appear to drive these patterns of diversity above and below ground, biological communities
461 respond in different ways and become increasingly decoupled as ecosystem development proceeds.

462

463 Of the various abiotic changes along the chronosequence, the long-term change in soil pH appears to be
464 the primary driver of community change for both prokaryotes and eukaryotes, although these groups
465 respond to long-term acidification in different ways. Plant diversity increases continuously during
466 ecosystem development along chronosequences worldwide (Laliberté et al., 2013), including the coastal
467 dunes at Jurien Bay (Laliberté, Zemunik & Turner, 2014; Zemunik et al., 2016), which is best explained by
468 long-term acidification and environmental filtering of the regional species pool dominated by plants
469 adapted to old, acidic, infertile soils (Laliberté, Zemunik & Turner, 2014). Similarly, fungal α -diversity
470 increased continuously along the chronosequence, driven primarily by the long-term decline in soil pH.
471 Soil pH is among the strongest abiotic correlates of fungal richness at the global scale (Tedersoo et al.,
472 2014), while a link between the species richness of plant and fungal communities has been reported
473 elsewhere at local, regional, and global scales (Peay, Baraloto & Fine, 2013; Tedersoo et al., 2014; Roy-
474 Bolduc et al., 2016). Soil pH also drives variation in bacterial community composition and diversity

475 across the globe, with greatest diversity at neutral to slightly acid pH (approximately pH 6 to 7) and a
476 marked reduction under strongly acidic and alkaline conditions (Lauber et al., 2009; Rousk et al., 2010;
477 Fierer, 2017). In agreement with the global pattern, bacterial α -diversity at Jurien Bay showed a
478 unimodal pattern with soil age, increasing on young soils, reaching a maximum on intermediate-aged
479 soils, and then declining to the lowest values on the old, most acidic soils (although these only reached
480 pH 6). Archaeal diversity followed a similar pattern according to the rarefied richness and Chao-1
481 indices, although it declined continuously for both the inverse Simpson and Shannon metrics.
482 Acidification associated with long-term pedogenesis therefore provides a unifying control on local
483 diversity of plant and microbial communities during long-term ecosystem development, although
484 prokaryotic and eukaryotic communities respond to soil pH change in different ways.

485
486 Despite the consistent response of above and below ground communities to long-term change in soil
487 pH, we found evidence for increasing decoupling of biological communities during the older stages of
488 ecosystem development. In other words, prokaryotic and eukaryotic communities change in a
489 coordinated manner during the early stages of ecosystem development in response to declining soil pH,
490 but become increasingly decoupled through time towards the late, retrogressive stages of ecosystem
491 development. A similar decoupling of change in the communities of plants and soil organisms, including
492 invertebrates, was observed recently in long-term retrogressive chronosequences in Australia and New
493 Zealand (Bokhorst et al., 2017). Although several studies have linked patterns of plant and microbial
494 diversity, there is evidence that bacteria and fungi respond to different drivers (Cline & Zak, 2015), and
495 overall associations remain unclear (Fierer & Jackson, 2006; Hendershot et al., 2017). Our results from
496 the Jurien Bay chronosequence therefore suggest that some of this variation might be linked to the
497 developmental stage of the ecosystem. For microbial communities, changes in the prokaryotic and
498 fungal communities became significantly more decoupled in older soils. The same was true for fungal
499 and vegetation communities, despite their similar patterns of α -diversity through time, demonstrating
500 that simple measures of local-scale diversity can mask a decoupling of community change.

501
502 In terms of symbiotic fungi, we found the greatest diversity of Glomeromycota in Middle Pleistocene
503 soils, supporting previous findings for arbuscular mycorrhizal fungi along the Jurien Bay chronosequence
504 that used a different locus to specifically target Glomeromycota (Krüger et al., 2015). However, we
505 found that the relative abundance of OTUs from this group was greater in young Holocene soils, where
506 their community composition differed from Pleistocene soils (Fig 3a,b), further supporting a decoupling

507 of plant and fungal diversity as ecosystem development proceeds. Although the fungal ITS primer we
508 used might lead to poor amplification of the Glomeromycota, there is support for its use in broad
509 studies of variation in the dominant taxa (Lekberg et al. 2018). For ectomycorrhizal fungi, Albornoz et al.
510 (2016) found that species richness of fungi infecting the roots of two co-occurring host plant species
511 declined along the chronosequence. This seems unlikely to be due to a reduction in potential fungal
512 partners given the increasing fungal diversity we detected here with soil age.

513
514 We assessed the influence of abiotic parameters on community composition in a variety of ways,
515 including redundancy analysis, regressions, PCA ordinations and multivariate regression trees, none of
516 which identified the large decline in soil phosphorus as a controlling factor. However, we cannot exclude
517 the possibility that changes in soil phosphorus also play a role in driving community change, because
518 strong co-variation between pH and phosphorus at Jurien Bay means that it is difficult to disentangle the
519 effects of these two properties along the chronosequence (Turner & Laliberté, 2015; Laliberté, Zemunik
520 & Turner, 2014; see below). Indeed, given that plants on the oldest soils at Jurien Bay are growing on
521 some of the lowest phosphorus soils in the world, and exhibit many mechanisms that allow them to
522 efficiently acquire and conserve phosphorus (Lambers et al., 2010; Zemunik et al., 2015), it seems likely
523 that many of the abundant microbes on the oldest soils are also well-adapted to the low-phosphorus
524 concentrations in their environment. Indeed, several studies have linked below-ground community
525 composition with fertility (e.g. Leff et al., 2015), including along retrogressive chronosequences of
526 marine terraces (Uroz et al., 2014) and post-glacial surfaces (Jangid et al., 2013). A number of bacterial
527 taxa increased markedly in abundance along the Jurien Bay chronosequence and reached their
528 maximum abundance on the oldest, most strongly weathered soils, indicating that these taxa are likely
529 to be extremely efficient at either acquiring or recycling phosphorus. As noted above, it is difficult to
530 isolate the influence of individual abiotic variables along the chronosequence, because pH and
531 phosphorus co-vary strongly. However, the soil pH reached only slightly to moderately acidic values and
532 varied relatively little among the older stages of the chronosequence (pH 6.0–6.4), while the old soils are
533 among the lowest phosphorus soils in the world (Yang et al., 2013; Turner & Laliberté, 2015). Indeed,
534 several bacteria increased markedly in abundance along the Jurien Bay sequence at resin phosphorus
535 concentrations $< 2 \text{ mg P kg}^{-1}$, which is a threshold that drives variation in above and below ground plant
536 and microbial communities in lowland tropical forests (Sheldrake et al., 2017; Turner, Brenes-Arguedas
537 & Condit, 2018; Yao et al., 2018). A role for phosphorus therefore seems likely, although experimental
538 work is required to isolate this from the overall decline in soil pH along the chronosequence.

539

540 The Verrucomicrobia have been identified previously as low fertility specialists (Fierer et al., 2013), in
541 particular the DA101 genus. At Jurien Bay, this organism increased markedly along the chronosequence,
542 eventually representing one of the most abundant bacterial OTU on the oldest soils. Its assignment as a
543 low phosphorus specialist is supported by the surprisingly small genome in members of this genus
544 (Brewer et al., 2016), which allows it to conserve phosphorus in particularly infertile environments. In
545 contrast, "*Candidatus Solibacter usitatus*", a species in the genus *Solibacter* that was also abundant on
546 the oldest soils, has a large genome that enables it to obtain a number of potentially limiting resources,
547 including phosphorus, which might also offer an advantage in low nutrient environments (Ward et al.,
548 2009; Challacombe et al., 2011). Indeed, members of the Solibacterales order in general appear to have
549 abundant genes for phosphatase enzyme synthesis and phosphorus solubilization (Bergkemper et al.,
550 2016). Given the vast diversity of phosphatase genes in microbes in low phosphorus soils (Yao et al.,
551 2018), organisms that are abundant on the old soils at Jurien Bay are likely to be particularly efficient at
552 phosphorus acquisition from extremely infertile environments. This provides important novel insight
553 into the ecology of these soil microbes and identifies them as potential targets for efforts to understand
554 biological adaptation to extreme nutrient stress.

555

556 **ACKNOWLEDGEMENTS**

557 We thank staff in the soils and sequencing labs at STRI, and Hans Lambers and Francois Teste for their
558 contributions. The research was funded by a grant from the Smithsonian Grand Challenges initiative to
559 the Life in the Cosmos program, an Australian Research Council (ARC) Discovery Early Career Researcher
560 Award (DECRA) to EL, and a University of Western Australia (UWA) Research Collaboration Award to EL
561 and BT. KS was supported financially by grant 429440 from the Simons Foundation to the Smithsonian
562 Tropical Research Institute (W. Wcislo, P.I.), and EL was supported by a NSERC Discovery Grant
563 (RGPIN-2014-06106). JJD was supported by by NASA contract NAS8-03060 to the Chandra X-ray Center.

564

565 **AUTHORS' CONTRIBUTIONS**

566

567

568 **DATA ACCESSIBILITY**

569 Data available from Figshare: <https://doi.org/10.6084/m9.figshare.7180388> (insert reference + citation)

570

571 **REFERENCES**

- 572 Abarenkov, K., Henrik, N. R., Larsson, K. H., Alexander, I. J., Eberhardt, U., Erland, S., Høiland, K., Kjøller,
573 R., Larsson, E., Pennanen, T., Sen, R., Taylor, A. F. S., Tedersoo, L., Ursing, B. M., Vrålstad, T.,
574 Liimatainen, K., Peintner, U. & Kõljalg, U. (2010) The UNITE database for molecular identification of
575 fungi – recent updates and future perspectives. *New Phytologist*, 186, 281-285.
- 576 Albornoz, F. E., Teste, F. P., Lambers, H., Bunce, M., Murray, D. C., White, N. E. & Laliberté, E. (2016)
577 Changes in ectomycorrhizal fungal community composition and declining diversity along a 2-million-
578 year soil chronosequence. *Molecular Ecology*, 25, 4919-4929.
- 579 Albuquerque, L., França, L., Rainey, F. A., Schumann, P., Nobre, M. F. & da Costa, M. S. (2011) *Gaiella*
580 *occulta* gen. nov., sp. nov., a novel representative of a deep branching phylogenetic lineage within
581 the class *Actinobacteria* and proposal of *Gaiellaceae* fam. nov. and *Gaiellales* ord. nov. *Systematic*
582 *and Applied Microbiology*, 34, 595-599.
- 583 Allison, V. J., Condron, L. M., Peltzer, D. A., Richardson, S. J. & Turner, B. L. (2007) Changes in enzyme
584 activities and soil microbial community composition along carbon and nutrient gradients at the Franz
585 Josef chronosequence, New Zealand. *Soil Biology & Biochemistry*, 39, 1770–1781.
- 586 Altschul, S. F., Gish, W., Miller, W., Myers, E. W. & Lipman, D. J. (1990) Basic local alignment search tool.
587 *Journal of Molecular Biology*, 215, 403-410.
- 588 Bergkemper, F., Schöler, A., Engel, M., Lang, F., Krüger, J., Schloter, M. & Schulz, S. (2016) Phosphorus
589 depletion in forest soils shapes bacterial communities towards phosphorus recycling systems.
590 *Environmental Microbiology*, 18, 1988-2000.
- 591 Birnbaum, C., Bissett, A., Teste, F. P. & Laliberté, E. (2018) Symbiotic N₂-fixer community composition,
592 but not diversity, shifts in nodules of a single host legume across a 2-million-year dune
593 chronosequence. *Microbial Ecology*, 76, 1009-1020.
- 594 Brewer, T. E., Handley, K. M., Carini, P., Gilbert, J. A. & Fierer, N. (2016) Genome reduction in an
595 abundant and ubiquitous soil bacterium ‘*Candidatus Udaeobacter copiosus*’. *Nature Microbiology*, 2,
596 16198.
- 597 Caporaso, J. G., Bittinger, K., Bushman, F. D., DeSantis, T. Z., Andersen, G. L. & Knight, R. (2010a) PyNAST:
598 a flexible tool for aligning sequences to a template alignment. *Bioinformatics*, 26, 266-267.
- 599 Caporaso, J. G., Kuczynski, J., Stombaugh, J., Bittinger, K., Bushman, F. D., Costello, E. K., Fierer, N., Peña,
600 A. G., Goodrich, J. K., Gordon, J. I., Huttley, G. A., Kelley, S. T., Knights, D., Koenig, J. E., Ley, R. E.,
601 Lozupone, C. A., McDonald, D., Muegge, B. D., Pirrung, M., Reeder, J., Sevinsky, J. R., Turnbaugh, P. J.,

602 Walters, W. A., Widmann, J., Yatsunenکو, T., Zaneveld, J. & Knight, R. (2010b) QIIME allows analysis
603 of high-throughput community sequencing data. *Nature Methods*, 7, 335-336.

604 Caporaso, J. G., Lauber, C. L., Walters, W. A., Berg-Lyons, D., Lozupone, C. A., Turnbaugh, P. J., Fierer, N.
605 & Knight, R. (2011) Global patterns of 16S rRNA diversity at a depth of millions of sequences per
606 sample. *Proceedings of the National Academy of Sciences*, 108, 4516-4522.

607 Castle, S. C., Nemergut, D. R., Grandy, A. S., Leff, J. W., Graham, E. B., Hood, E., Schmidt, S. K., Wickings,
608 K. & Cleveland, C. C. (2016) Biogeochemical drivers of microbial community convergence across
609 actively retreating glaciers. *Soil Biology & Biochemistry*, 101, 74-84.

610 Challacombe, J. F., Eichorst, S. A., Hauser, L., Land, M., Xie, G. & Kuske, C. R. (2011) Biological
611 consequences of ancient gene acquisition and duplication in the large genome of *Candidatus*
612 *Solibacter usitatus* Ellin6076. *PLOS ONE*, 6, e24882.

613 Chao, A. (1984) Nonparametric estimation of the number of classes in a population. *Scandinavian*
614 *Journal of Statistics*, 11, 265-270.

615 Cline, L. C. & Zak, D. R. (2015) Soil microbial communities are shaped by plant-driven changes in
616 resource availability during secondary succession. *Ecology*, 96, 3374-3385.

617 Coomes, D., Bentley, W., Tanentzap, A. & Burrows, L. (2013) Soil drainage and phosphorus depletion
618 contribute to retrogressive succession along a New Zealand chronosequence. *Plant and Soil*, 367, 77-
619 91.

620 Cutler, N. A., Chaput, D. L. & van der Gast, C. J. (2014) Long-term changes in soil microbial communities
621 during primary succession. *Soil Biology & Biochemistry*, 69, 359-370.

622 Delgado-Baquerizo, M., Oliverio, A. M., Brewer, T. E., Benavent-González, A., Eldridge, D. J., Bardgett, R.
623 D., Maestre, F. T., Singh, B. K. & Fierer, N. (2018) A global atlas of the dominant bacteria found in soil.
624 *Science*, 359, 320-325.

625 Edgar, R. C. (2010) Search and clustering orders of magnitude faster than BLAST. *Bioinformatics*, 26,
626 2460-2461.

627 Fierer, N., Ladau, J., Clemente, J. C., Leff, J. W., Owens, S. M., Pollard, K. S., Knight, R., Gilbert, J. A. &
628 McCulley, R. L. (2013) Reconstructing the microbial diversity and function of pre-agricultural tallgrass
629 prairie soils in the United States. *Science*, 342, 621-624.

630 Fierer, N. (2017) Embracing the unknown: disentangling the complexities of the soil microbiome. *Nature*
631 *Reviews Microbiology*, 15, 579-590.

- 632 Hayes, P., Turner, B. L., Lambers, H. & Laliberté, E. (2014) Foliar nutrient concentrations and resorption
633 efficiency in plants of contrasting nutrient-acquisition strategies along a 2-million-year dune
634 chronosequence. *Journal of Ecology*, 102, 396-410.
- 635 Hendershot, J. N., Read, Q. D., Henning, J. A., Sanders, N. J. & Classen, A. T. (2017) Consistently
636 inconsistent drivers of microbial diversity and abundance at macroecological scales. *Ecology*, 98,
637 1757-1763.
- 638 Hendershot, W. H., Lalande, H. & Duquette, M. (2008) Chapter 18. Ion exchange and exchangeable
639 cations. *Soil Sampling and Methods of Analysis* (eds M.R. Carter & E. Gregorich), pp. 173-178.
640 Canadian Society of Soil Science and CRC Press, Boca Raton, FL.
- 641 Hopper, S. D. (2014) Sandplain and Kwongan: historical spellings, meanings, synonyms, geography and
642 definition. *Plant life on the sandplains in Southwest Australia, a global biodiversity hotspot* (ed. H.
643 Lambers). UWA Publishing, Crawley, Australia.
- 644 Jangid, K., Whitman, W. B., Condon, L. M., Turner, B. L. & Williams, M. A. (2013) Soil bacterial
645 community succession during long-term ecosystem development. *Molecular Ecology*, 22, 3415–3424.
- 646 Kardol, P. & Wardle, D. A. (2010) How understanding aboveground–belowground linkages can assist
647 restoration ecology. *Trends in Ecology & Evolution*, 25, 670-679.
- 648 Kendrick, G. W., Wyrwoll, K.-H. & Szabo, B. J. (1991) Pliocene-Pleistocene coastal events and history
649 along the western margin of Australia. *Quaternary Science Reviews*, 10, 419-439.
- 650 Kim, M. K., Na, J.-R., Lee, T.-H., Im, W.-T., Soung, N.-K. & Yang, D.-C. (2007) *Solirubrobacter soli* sp. nov.,
651 isolated from soil of a ginseng field. *International Journal of Systematic and Evolutionary*
652 *Microbiology*, 57, 1453-1455.
- 653 Krüger, M., Teste, F. P., Laliberté, E., Lambers, H., Coghlan, M., Zemunik, G. & Bunce, M. (2015) The rise
654 and fall of arbuscular mycorrhizal fungal diversity during ecosystem retrogression. *Molecular Ecology*,
655 24, 4912-4930.
- 656 Laliberté, E., Grace, J. B., Huston, M. A., Lambers, H., Teste, F. P., Turner, B. L. & Wardle, D. A. (2013)
657 How does pedogenesis drive plant diversity? *Trends in Ecology & Evolution*, 28, 331–340.
- 658 Laliberté, E., Kardol, P., Didham, R. K., Teste, F. P., Turner, B. L. & Wardle, D. A. (2017) Soil fertility
659 shapes belowground food webs across a regional climate gradient. *Ecology Letters*, 20, 1273-1284.
- 660 Laliberté, E., Turner, B. L., Costes, T., Pearse, S. J., Wyrwoll, K.-H., Zemunik, G. & Lambers, H. (2012)
661 Experimental assessment of nutrient limitation along a 2-million-year dune chronosequence in the
662 south-western Australia biodiversity hotspot. *Journal of Ecology*, 100, 631-642.

663 Laliberté, E., Zemunik, G. & Turner, B. L. (2014) Environmental filtering explains variation in plant
664 diversity along resource gradients. *Science*, 345, 1602-1605.

665 Lambers, H., Ahmedi, I., Berkowitz, O., Dunne, C., Finnegan, P. M., St J. Hardy, G. E., Jost, R., Laliberté, E.,
666 S.J., P. & Teste, F. P. (2013) Phosphorus nutrition of phosphorus-sensitive Australian native plants:
667 threats to plant communities in a global biodiversity hotspot. *Conservation Physiology*, 1, cot010
668 (2013). doi: 2010.1093/conphys/cot2010.

669 Lambers, H., Brundrett, M. C., Raven, J. A. & Hopper, S. D. (2010) Plant mineral nutrition in ancient
670 landscapes: high plant species diversity on infertile soils is linked to functional diversity for nutritional
671 strategies. *Plant and Soil*, 334, 11-31.

672 Lamont, B. B., Hopkins, A. J. M. & Hnatiuk, R. J. (1984) The flora - composition, diversity and origins.
673 *Kwongan: Plant Life of the Sandplain* (eds J.S. Pate & J.S. Beard), pp. 27–50. University of Western
674 Australia Press, Nedlands, Western Australia.

675 Lauber, C. L., Hamady, M., Knight, R. & Fierer, N. (2009) Pyrosequencing-based assessment of soil pH as
676 a predictor of soil bacterial community structure at the continental scale. *Applied and Environmental*
677 *Microbiology*, 75, 5111-5120.

678 Leff, J. W., Jones, S. E., Prober, S. M., Barberán, A., Borer, E. T., Firn, J. L., Harpole, W. S., Hobbie, S. E.,
679 Hofmockel, K. S., Knops, J. M. H., McCulley, R. L., La Pierre, K., Risch, A. C., Seabloom, E. W., Schütz,
680 M., Steenbock, C., Stevens, C. J. & Fierer, N. (2015) Consistent responses of soil microbial
681 communities to elevated nutrient inputs in grasslands across the globe. *Proceedings of the National*
682 *Academy of Sciences*, 112, 10967-10972.

683 Lekberg, Y., Vasar, M., Bullington, L.S., Sepp, S.-K., Antunes, P.M., Bunn, R., Larkin, B. G., & Ópik, M.
684 (2018) More bang for the buck? Can arbuscular mycorrhizal communities be characterized
685 adequately alongside other fungi using general fungal primers? *New Phytologist*, 220, 971–976.

686 Lisboa, F. J. G., Peres-Neto, P. R., Chaer, G. M., Jesus, E. d. C., Mitchell, R. J., Chapman, S. J. & Berbara, R.
687 L. L. (2014) Much beyond Mantel: Bringing Procrustes association metric to the plant and soil
688 ecologist's toolbox. *PLOS ONE*, 9, e101238.

689 Loeppert, R. H. & Inskeep, W. P. (1996) Iron. *Methods of Soil Analysis, Part 3 – Chemical Methods* (eds
690 D.L. Sparks & e. al.), pp. 639–664. Soil Science Society of America, Madison, WI.

691 Magurran, A.E. (2004) *Measuring Biological Diversity*. Blackwell Science, Oxford, UK.

692 McDonald, D., Price, M. N., Goodrich, J., Nawrocki, E. P., DeSantis, T. Z., Probst, A., Andersen, G. L.,
693 Knight, R. & Hugenholtz, P. (2012) An improved Greengenes taxonomy with explicit ranks for
694 ecological and evolutionary analyses of bacteria and archaea. *The ISME Journal*, 6, 610-618.

695 Myers, N., Mittermeier, R. A., Mittermeier, C. G., da Fonseca, G. A. B. & Kent, J. (2000) Biodiversity
696 hotspots for conservation priorities. *Nature*, 403, 853-858.

697 Peay, K. G., Baraloto, C. & Fine, P. V. A. (2013) Strong coupling of plant and fungal community structure
698 across western Amazonian rainforests. *The ISME Journal*, 7, 1852-1861.

699 Prober, S. M., Leff, J. W., Bates, S. T., Borer, E. T., Firn, J., Harpole, W. S., Lind, E. M., Seabloom, E. W.,
700 Adler, P. B., Bakker, J. D., Cleland, E. E., DeCrappeo, N. M., DeLorenze, E., Hagenah, N., Hautier, Y.,
701 Hofmockel, K. S., Kirkman, K. P., Knops, J. M. H., La Pierre, K. J., MacDougall, A. S., McCulley, R. L.,
702 Mitchell, C. E., Risch, A. C., Schuetz, M., Stevens, C. J., Williams, R. J. & Fierer, N. (2015) Plant diversity
703 predicts beta but not alpha diversity of soil microbes across grasslands worldwide. *Ecology Letters*,
704 18, 85-95.

705 Rousk, J., Baath, E., Brookes, P. C., Lauber, C. L., Lozupone, C., Caporaso, J. G., Knight, R. & Fierer, N.
706 (2010) Soil bacterial and fungal communities across a pH gradient in an arable soil. *ISME Journal*, 4,
707 1340-1351.

708 Roy-Bolduc, A., Laliberté, E., Boudreau, S. & Hijri, M. (2016) Strong linkage between plant and soil fungal
709 communities along a successional coastal dune system. *FEMS Microbiology Ecology*, 92, fiw156,
710 <https://doi.org/10.1093/femsec/fiw156>

711 Sait, M., Hugenholtz, P. & Janssen, P. H. (2002) Cultivation of globally distributed soil bacteria from
712 phylogenetic lineages previously only detected in cultivation-independent surveys. *Environmental*
713 *Microbiology*, 4, 654-666.

714 Shane, M. W. & Lambers, H. (2005) Cluster roots: A curiosity in context. *Plant and Soil*, 274, 101-125.

715 Sheldrake, M., Rosenstock, N. P., Revillini, D., Olsson, P. A., Wright, S. J. & Turner, B. L. (2017) A
716 phosphorus threshold for mycoheterotrophic plants in tropical forests. *Proceedings of the Royal*
717 *Society B: Biological Sciences*, 284.

718 Stevens, P. R. & Walker, T. W. (1970) The chronosequence concept and soil formation. *The Quarterly*
719 *Review of Biology*, 45, 333-350.

720 Tarlera, S., Jangid, K., Ivester, A. H., Whitman, W. B. & Williams, M. A. (2008) Microbial community
721 succession and bacterial diversity in soils during 77 000 years of ecosystem development. *FEMS*
722 *Microbiol Ecology*, 64, 129-140.

723 Tedersoo, L., Bahram, M., Pöhlme, S., Kõljalg, U., Yorou, N. S., Wijesundera, R., Ruiz, L. V., Vasco-Palacios,
724 A. M., Thu, P. Q., Suija, A., Smith, M. E., Sharp, C., Saluveer, E., Saitta, A., Rosas, M., Riit, T.,
725 Ratkowsky, D., Pritsch, K., Pöldmaa, K., Piepenbring, M., Phosri, C., Peterson, M., Parts, K., Pärtel, K.,
726 Otsing, E., Nouhra, E., Njouonkou, A. L., Nilsson, R. H., Morgado, L. N., Mayor, J., May, T. W.,

727 Majuakim, L., Lodge, D. J., Lee, S. S., Larsson, K.-H., Kohout, P., Hosaka, K., Hiiesalu, I., Henkel, T. W.,
728 Harend, H., Guo, L.-d., Greslebin, A., Grelet, G., Geml, J., Gates, G., Dunstan, W., Dunk, C., Drenkhan,
729 R., Dearnaley, J., De Kesel, A., Dang, T., Chen, X., Buegger, F., Brearley, F. Q., Bonito, G., Anslan, S.,
730 Abell, S. & Abarenkov, K. (2014) Global diversity and geography of soil fungi. *Science*, 346.

731 Thompson, L. R., Sanders, J. G., McDonald, D., Amir, A., Ladau, J., Locey, K. J., Prill, R. J., Tripathi, A.,
732 Gibbons, S. M., Ackermann, G., Navas-Molina, J. A., Janssen, S., Kopylova, E., Vázquez-Baeza, Y.,
733 González, A., Morton, J. T., Mirarab, S., Zech Xu, Z., Jiang, L., Haroon, M. F., Kanbar, J., Zhu, Q., Jin
734 Song, S., Kosciółek, T., Bokulich, N. A., Lefler, J., Brislawn, C. J., Humphrey, G., Owens, S. M.,
735 Hampton-Marcell, J., Berg-Lyons, D., McKenzie, V., Fierer, N., Fuhrman, J. A., Clauset, A., Stevens, R.
736 L., Shade, A., Pollard, K. S., Goodwin, K. D., Jansson, J. K., Gilbert, J. A., Knight, R. & The Earth
737 Microbiome Project, C. (2017) A communal catalogue reveals Earth's multiscale microbial diversity.
738 *Nature*, 551, 457.

739 Turner, B. L., Brenes-Arguedas, T. & Condit, R. (2018) Pervasive phosphorus limitation of tree species but
740 not communities in tropical forests. *Nature*, 555, 367.

741 Turner, B. L., Hayes, P. E. & Laliberté, E. (2018) A climosequence of chronosequences in southwestern
742 Australia. *European Journal of Soil Science*, 69, 69-85.

743 Turner, B. L. & Laliberté, E. (2015) Soil development and nutrient availability along a 2 million-year
744 coastal dune chronosequence under species-rich Mediterranean shrubland in southwestern
745 Australia. *Ecosystems*, 18, 287-309.

746 Turner, B. L. & Romero, T. E. (2009) Short-term changes in extractable inorganic nutrients during storage
747 of tropical rain forest soils. *Soil Science Society of America Journal*, 73, 1972-1979.

748 Turner, S., Mikutta, R., Meyer-Stüve, S., Guggenberger, G., Schaarschmidt, F., Lazar, C. S., Dohrmann, R.
749 & Schippers, A. (2017) Microbial community dynamics in soil depth profiles over 120,000 years of
750 ecosystem development. *Frontiers in Microbiology*, 8, <https://doi.org/10.3389/fmicb.2017.00874>

751 Uroz, S., Tech, J. J., Sawaya, N. A., Frey-Klett, P. & Leveau, J. H. J. (2014) Structure and function of
752 bacterial communities in ageing soils: Insights from the Mendocino ecological staircase. *Soil Biology &*
753 *Biochemistry*, 69, 265-274.

754 Vitousek, P. M. & Farrington, H. (1997) Nutrient limitation and soil development: Experimental test of a
755 biogeochemical theory. *Biogeochemistry*, 37, 63-75.

756 Walker, L. R., Wardle, D. A., Bardgett, R. D. & Clarkson, B. D. (2010) The use of chronosequences in
757 studies of ecological succession and soil development. *Journal of Ecology*, 98, 725-736.

- 758 Walker, T. W. & Adams, A. F. R. (1958) Studies on soil organic matter: I. influence of phosphorus content
759 of parent materials on accumulations of carbon, nitrogen, sulfur, and organic phosphorus in
760 grassland soils. *Soil Science*, 85, 307-318.
- 761 Ward, N. L., Challacombe, J. F., Janssen, P. H., Henrissat, B., Coutinho, P. M., Wu, M., Xie, G., Haft, D. H.,
762 Sait, M., Badger, J., Barabote, R. D., Bradley, B., Brettin, T. S., Brinkac, L. M., Bruce, D., Creasy, T.,
763 Daugherty, S. C., Davidsen, T. M., DeBoy, R. T., Detter, J. C., Dodson, R. J., Durkin, A. S., Ganapathy, A.,
764 Gwinn-Giglio, M., Han, C. S., Khouri, H., Kiss, H., Kothari, S. P., Madupu, R., Nelson, K. E., Nelson, W.
765 C., Paulsen, I., Penn, K., Ren, Q., Rosovitz, M. J., Selengut, J. D., Shrivastava, S., Sullivan, S. A., Tapia,
766 R., Thompson, L. S., Watkins, K. L., Yang, Q., Yu, C., Zafar, N., Zhou, L. & Kuske, C. R. (2009) Three
767 genomes from the phylum Acidobacteria provide insight into the lifestyles of these microorganisms in
768 soils. *Applied and Environmental Microbiology*, 75, 2046-2056.
- 769 Wardle, D. A., Walker, L. R. & Bardgett, R. D. (2004) Ecosystem properties and forest decline in
770 contrasting long-term chronosequences. *Science*, 305, 509-513.
- 771 White, T. J., Bruns, T., Lee, S. & Taylor, J. (1990) Amplification and direct sequencing of fungal ribosomal
772 RNA genes for phylogenetics. *PCR Protocols: a Guide to Methods and Applications* (eds M.A. Innis,
773 D.H. Gelfand, J.J. Sninsky & T.J. White), pp. 315-322. Academic Press, New York.
- 774 Williamson, W. M., Wardle, D. A. & Yeates, G. W. (2005) Changes in soil microbial and nematode
775 communities during ecosystem decline across a long-term chronosequence. *Soil Biology &*
776 *Biochemistry*, 37, 1289-1301.
- 777 Wyrwoll, K.-H., Turner, B. L. & Findlater, P. (2014) On the origins, geomorphology and soils of the
778 sandplains of south-western Australia. *Plant Life on the Sandplains in Southwest Australia, a Global*
779 *Biodiversity Hotspot* (ed. H. Lambers). University of Western Australia, Crawley, Australia.
- 780 Yang, X., Post, W. M., Thornton, P. E. & Jain, A. (2013) The distribution of soil phosphorus for global
781 biogeochemical modeling. *Biogeosciences*, 10, 2525-2537.
- 782 Yao, Q., Li, Z., Song, Y., Wright, S. J., Guo, X., Tringe, S. G., Tfaily, M. M., Paša-Tolić, L., Hazen, T. C.,
783 Turner, B. L., Mayes, M. A. & Pan, C. (2018) Community proteogenomics reveals the systemic impact
784 of phosphorus availability on microbial functions in tropical soil. *Nature Ecology & Evolution*, 2, 499-
785 509.
- 786 Zemunik, G., Turner, B. L., Lambers, H. & Laliberté, E. (2015) Diversity of plant nutrient-acquisition
787 strategies increases during long-term ecosystem development. *Nature Plants*, 1, 15050.

788 Zemunik, G., Turner, B. L., Lambers, H. & Laliberté, E. (2016) Increasing plant species diversity and
789 extreme species turnover accompany declining soil fertility along a long-term chronosequence in a
790 biodiversity hotspot. *Journal of Ecology*, 104, 792-805.

791 Zhou, J., Deng, Y., Shen, L., Wen, C., Yan, Q., Ning, D., Qin, Y., Xue, K., Wu, L., He, Z., Voordeckers, J. W.,
792 Nostrand, J. D. V., Buzzard, V., Michaletz, S. T., Enquist, B. J., Weiser, M. D., Kaspari, M., Waide, R.,
793 Yang, Y. & Brown, J. H. (2016) Temperature mediates continental-scale diversity of microbes in forest
794 soils. *Nature Communications*, 7, 12083.

Author Manuscript

Table 1. Soil properties along the Jurien Bay chronosequence. Values are means \pm standard deviation of five plots on each chronosequence stage. ECEC, effective cation exchange capacity; NO₃, nitrate. Chronosequence stages are based on the numbering system established previously (Laliberté *et al.* 2012; Turner & Laliberté 2015).

Chronosequence stage	2	3	4	5	6
Dune formation	Quindalup	Quindalup	Spearwood	Spearwood	Bassendean
Geological period	Holocene	Holocene	Middle Pleistocene	Middle Pleistocene	Early Pleistocene
Approximate age (years)	100-1000	6500	120,000	200-400,000	2,000,000
Soil pH (water)	8.6 \pm 0.1	8.6 \pm 0.1	6.4 \pm 0.1	6.4 \pm 0.3	6.0 \pm 0.2
Carbonate (%)	77 \pm 7	22 \pm 11	0	0	0
Organic C (%)	1.87 \pm 0.74	1.16 \pm 0.25	0.69 \pm 0.14	0.40 \pm 0.07	0.53 \pm 0.22
Total N (%)	0.115 \pm 0.014	0.069 \pm 0.010	0.026 \pm 0.005	0.011 \pm 0.003	0.019 \pm 0.010
Total P (mg P kg ⁻¹)	429 \pm 38	187 \pm 62	20.2 \pm 3.1	8.4 \pm 2.2	5.2 \pm 1.2
Resin P (mg P kg ⁻¹)	4.38 \pm 2.52	1.67 \pm 0.17	0.93 \pm 0.17	0.53 \pm 0.08	0.73 \pm 0.09
Extractable NO ₃ (mg N kg ⁻¹)	4.3 \pm 1.5	2.7 \pm 1.5	0.9 \pm 0.4	0.7 \pm 0.5	0.8 \pm 0.6
ECEC (cmol _c kg ⁻¹)	11.4 \pm 2.7	10.5 \pm 1.7	3.3 \pm 0.4	1.9 \pm 0.2	2.4 \pm 0.6

Table 2. Mean number \pm standard deviation of sequences per sample, total OTUs found, and α -diversity calculated by observed OTUs and the Chao-1 estimator for five stages of the Jurien Bay chronosequence. Rarefaction levels for α -diversity calculations using QIIME 1.9.1: Archaea 570, bacteria 58,400, fungi 34,000. Diversity values are mean \pm standard deviation of four (stages 2 and 3) or five (stages 4-6) replicate plots at each stage. For Observed OTUs and Chao-1, values with the same letter are not significantly different ($p > 0.05$)

Chronosequence stage	2	3	4	5	6
Dune formation	Quindalup	Quindalup	Spearwood	Spearwood	Bassendean
Approximate age (years)	100-1000	6500	120,000	200-400,000	2,000,000

Archaea (16S)

Mean No. of Seqs	3522 ± 1524	5687 ± 2878	1437 ± 532	1777 ± 718	1084 ± 430
Total OTUs	101	76	101	88	65
Observed OTUs	20 ± 1 ^{ac}	22 ± 3 ^{ac}	29 ± 3 ^{bc}	23 ± 5 ^c	20 ± 4 ^{abc}
Chao-1	33 ± 6 ^{ac}	34 ± 5 ^{ac}	47 ± 5 ^{bc}	35 ± 5 ^c	27 ± 6 ^{ac}
Bacteria (16S)					
Mean No. of Seqs	112,393 ± 56,033	137,966 ± 48,435	235,018 ± 64,155	288,403 ± 72,195	248,106 ± 21,909
Total OTUs	20,254	18,285	32,863	34,796	28,925
Observed OTUs	7478 ± 96 ^a	7688 ± 386 ^a	8265 ± 417 ^a	7749 ± 460 ^a	6918 ± 487 ^a
Chao-1	12,100 ± 407 ^a	12,980 ± 914 ^a	13,770 ± 939 ^a	13,181 ± 706 ^a	11,397 ± 599 ^a
Fungi (ITS)					
Mean No. of Seqs	64,263 ± 24,092	53,337 ± 21,320	77,857 ± 13,379	66,885 ± 13422	71,587 ± 19,950
Total OTUs	2335	2406	6173	6314	6849
Observed OTUs	817 ± 90 ^a	926 ± 81 ^{ab}	1540 ± 373 ^{ab}	1626 ± 234 ^{ab}	1805 ± 104 ^b
Chao-1	1064 ± 107 ^{ab}	1157 ± 118 ^b	2103 ± 474 ^{ab}	2186 ± 385 ^{ab}	2389 ± 157 ^a

Table 3. Biological community change along the Jurien Bay chronosequence. For microbes, only abundant phyla are shown (> 0.5% of total OTUs). Values are mean percent relative abundance ± standard deviation of five plots on each chronosequence stage (four plots on the Holocene Quindalup dunes). Mean relative cover (%) is shown for the seven plant families with greatest canopy cover.

Chronosequence stage	2	3	4	5	6
Dune formation	Quindalup	Quindalup	Spearwood	Spearwood	Bassendean
Approximate age (years)	100-1000	6500	120,000	200-400,000	2,000,000
Archaea (16S)					
Crenarchaeota	3.0 ± 0.6	3.9 ± 0.7	0.6 ± 0.2	0.6 ± 0.2	0.4 ± 0.2
Bacteria (16S)					
Acidobacteria	10.4 ± 1.5	13.4 ± 1.0	13.1 ± 1.8	13.8 ± 1.0	15.4 ± 0.7
Actinobacteria	26.6 ± 1.8	26.4 ± 2.5	28.9 ± 3.9	26.0 ± 3.9	24.7 ± 4.7
Bacteroidetes	6.2 ± 0.7	4.1 ± 0.5	5.2 ± 1.1	4.0 ± 1.2	4.0 ± 0.6
Chloroflexi	3.1 ± 0.2	3.1 ± 0.2	3.1 ± 0.6	2.8 ± 1.0	1.9 ± 0.6
Firmicutes	1.1 ± 0.4	0.9 ± 0.4	1.1 ± 0.3	0.9 ± 0.3	0.9 ± 0.3
Gemmatimonadetes	5.3 ± 0.7	5.8 ± 1.0	2.8 ± 1.2	2.6 ± 1.4	1.3 ± 0.7
Nitrospirae	0.9 ± 0.1	1.3 ± 0.2	0.3 ± 0.1	0.3 ± 0.2	0.1 ± 0.1
Planctomycetes	5.8 ± 1.1	5.9 ± 0.7	5.3 ± 1.0	6.8 ± 2.3	6.9 ± 1.0
Proteobacteria	32.0 ± 1.2	29.3 ± 1.0	33.5 ± 1.8	31.1 ± 4.5	32.2 ± 2.2
Verrucomicrobia	3.2 ± 0.5	3.1 ± 0.5	5.9 ± 0.9	6.8 ± 0.8	7.0 ± 1.5

WPS-2	<0.1	<0.1	0.1 ± 0.3	0.3 ± 0.1	1.2 ± 0.8
Fungi (ITS)					
Ascomycota	26.7 ± 5.1	40.7 ± 7.7	54.8 ± 11.2	50.9 ± 15.5	39.6 ± 7.8
Basidiomycota	12.9 ± 6.0	9.5 ± 2.2	22.1 ± 8.5	22.9 ± 14.2	17.2 ± 6.8
Chytridiomycota	1.2 ± 1.6	0.3 ± 0.1	0.2 ± 0.2	0.2 ± 0.2	0.4 ± 0.3
Glomeromycota	0.4 ± 0.6	0.4 ± 0.3	0.2 ± 0.1	0.2 ± 0.1	0.1 ± 0.1
Zygomycota	2.2 ± 0.5	3.1 ± 2.9	0.7 ± 0.3	2.0 ± 2.9	1.6 ± 1.3
Unidentified	56.4 ± 11.6	45.9 ± 8.1	21.6 ± 12.5	23.4 ± 7.3	40.4 ± 12.7
Plants					
Cyperaceae	1.4 ± 1.4	5.4 ± 2.0	2.8 ± 1.7	14.4 ± 3.5	7.8 ± 3.5
Dilleniaceae	0	0	20.4 ± 16.3	7.4 ± 4.8	4.3 ± 4.7
Fabaceae	13.8 ± 11.8	13.0 ± 10.4	5.5 ± 4.5	3.7 ± 6.0	20.1 ± 13.6
Haemodoraceae	8.2 ± 4.8	6.5 ± 4.2	4.5 ± 1.4	2.3 ± 2.2	4.5 ± 1.4
Myrtaceae	29.1 ± 9.5	29.9 ± 11.9	20.9 ± 13.4	32.6 ± 24.2	19.4 ± 7.0
Proteaceae	0	0	36.3 ± 24.2	28.6 ± 9.5	28.0 ± 14.9
Restionaceae	12.1 ± 8.6	16.3 ± 12.0	4.0 ± 2.5	3.3 ± 1.2	2.2 ± 0.7

Figure 1. Changes in the relative abundance of selected bacterial taxa along the Jurien Bay chronosequence, showing (a) classes within the phylum Proteobacteria, (b) orders within the class Alphaproteobacteria. Values are means ± standard deviation of five plots on each chronosequence stage (four plots on the Holocene dunes). Approximate soil ages are shown in the x axis.

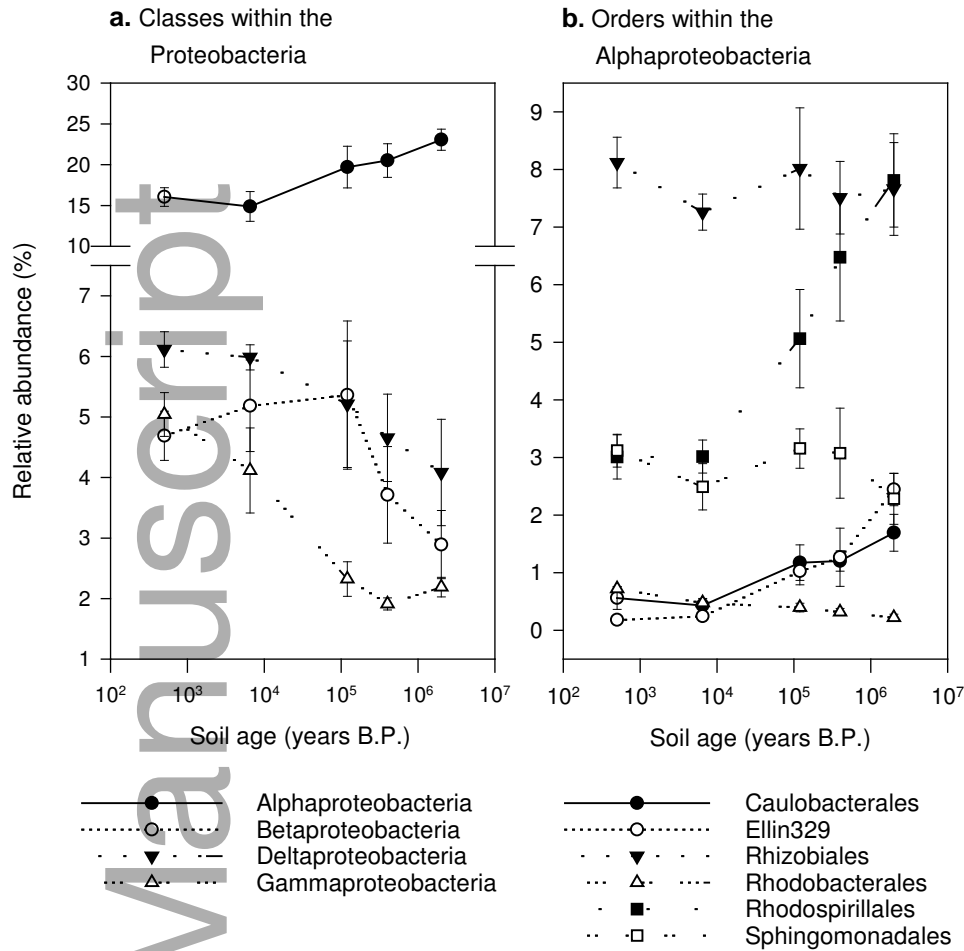
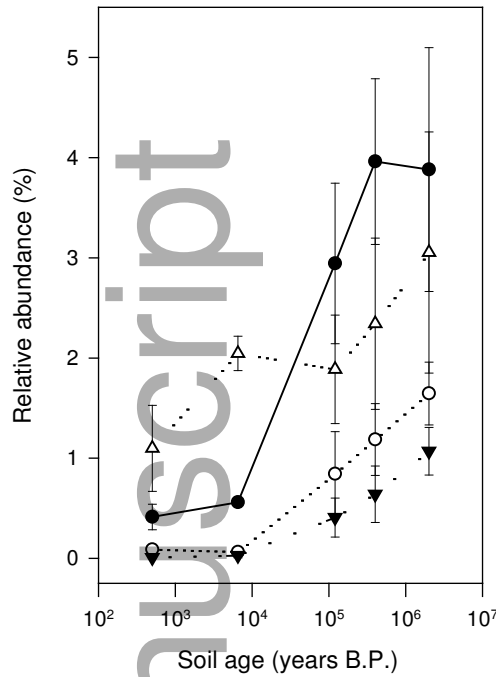


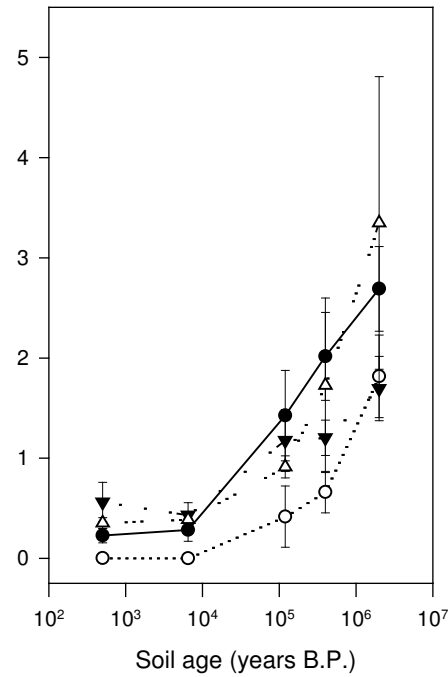
Figure 2. Changes in the relative abundance of (a) genera, and (b) families of bacteria that were more abundant on the old, low phosphorus soils. Values are means \pm standard deviation of five plots on each chronosequence stage (four plots on the Holocene dunes).

a. Low phosphorus genera



● DA101 (Verrucomicrobia)
 ○ Candidatus Solibacter
 ▼ Candidatus Koribacter
 △ Gaiella (Actinobacteria)

b. Low phosphorus families



● Acetobacteraceae
 ○ Acidobacteriaceae
 ▼ Caulobacteraceae
 △ Conexibacteraceae

Figure 3. Changes in the relative abundance of (a) total fungal OTUs in the phylum Glomeromycota, (b) two families of fungi in the Glomeromycota exhibiting different patterns along the chronosequence, and (c) families containing bacteria that fix nitrogen. In (c) only families containing a number of nitrogen-fixing genera are shown, in addition to the genus *Frankia*. Values are means \pm standard deviation of five plots on each chronosequence stage (four plots on the Holocene dunes).

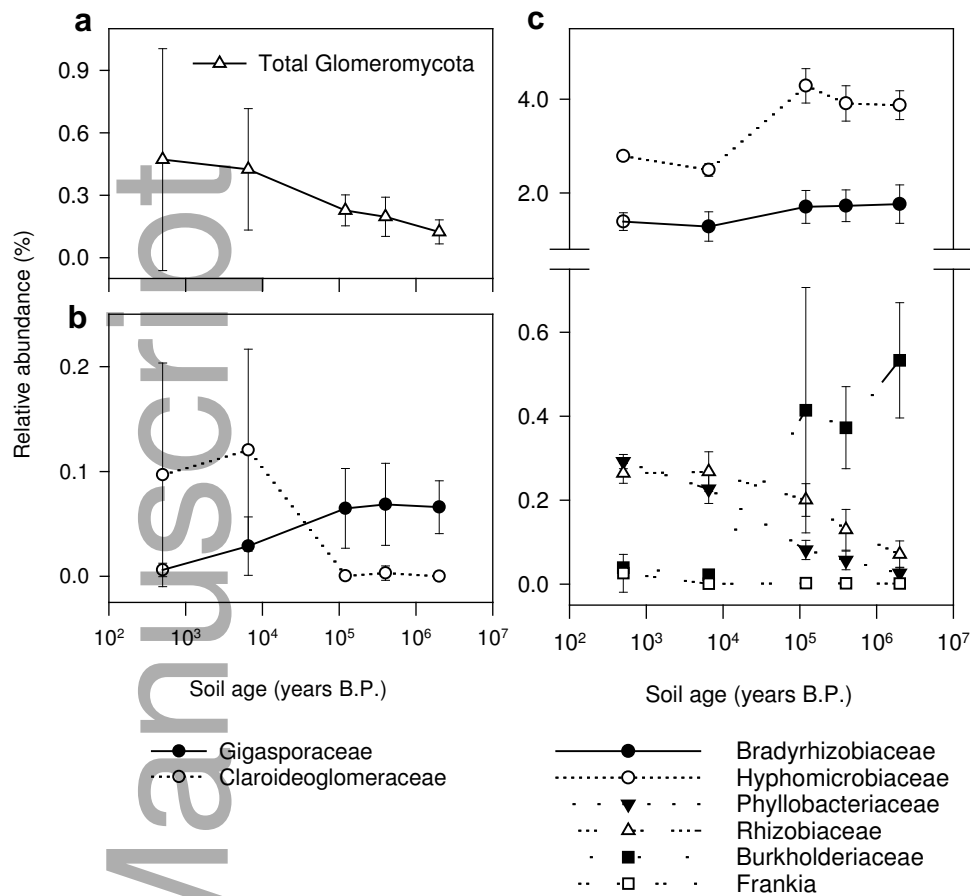


Figure 4. Rarefied richness (a–d), Simpson (1/D) diversity (e–h), and Shannon diversity (i–l) for fungi (a, e, i), bacteria (b, f, j), archaea (c, g, k) and plants (d, h, l) along the Jurien Bay chronosequence. The boxes contain all values within the 25th and 75th percentiles, the whiskers extend to 150% of the interquartile range from the box, and outliers are represented by dots.

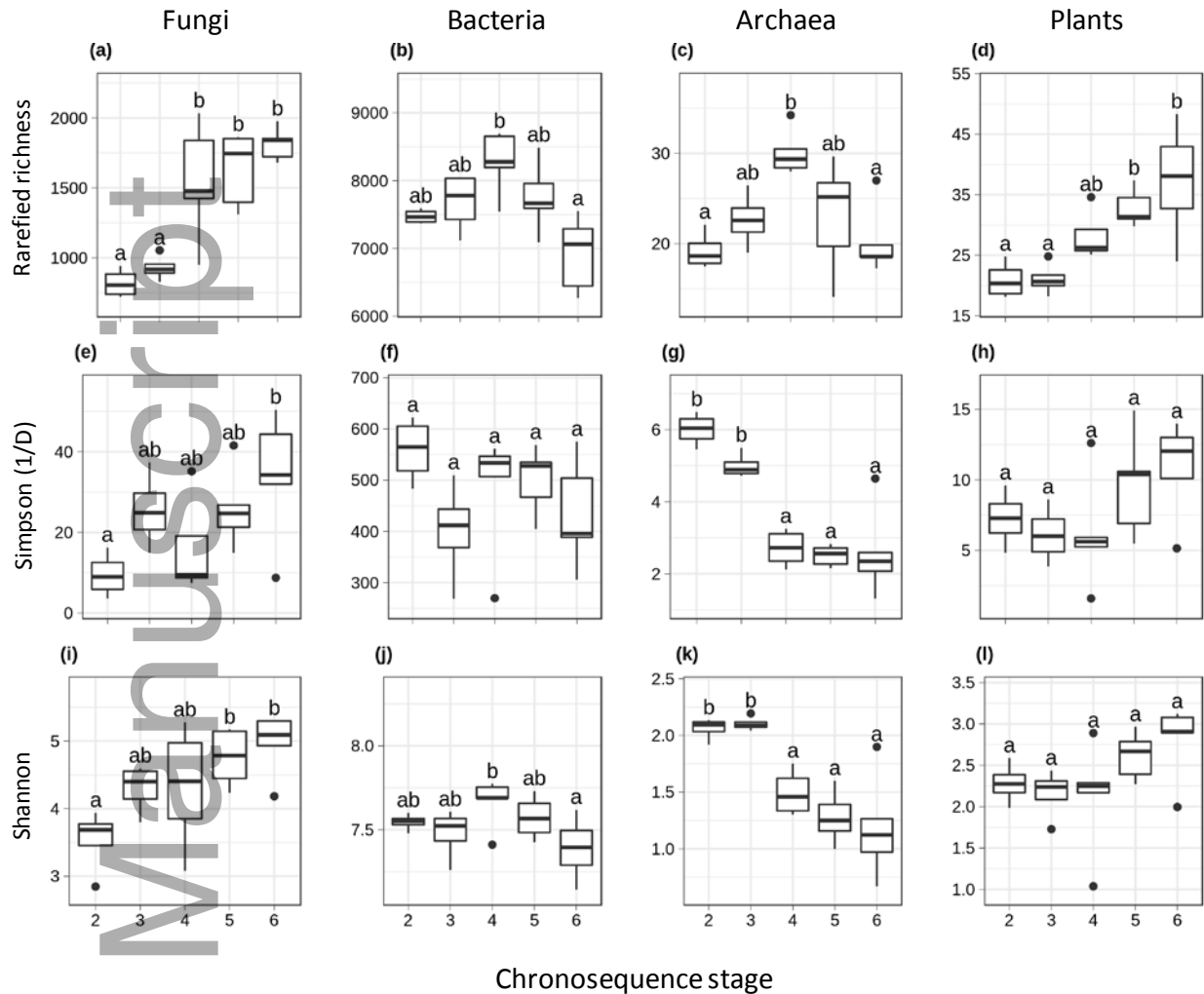


Figure 5. NMDS ordinations of biological communities along the Jurien Bay chronosequence, showing (a) the 16S (bacteria and archaea) community data with logbase of the modified Gower distance set to 2 (stress 0.05), (b), fungal community data with logbase of the modified Gower distance set to 2 (stress 0.11), (c) the vegetation community (relative cover) with logbase of the modified Gower distance set to 2 (stress 0.10).

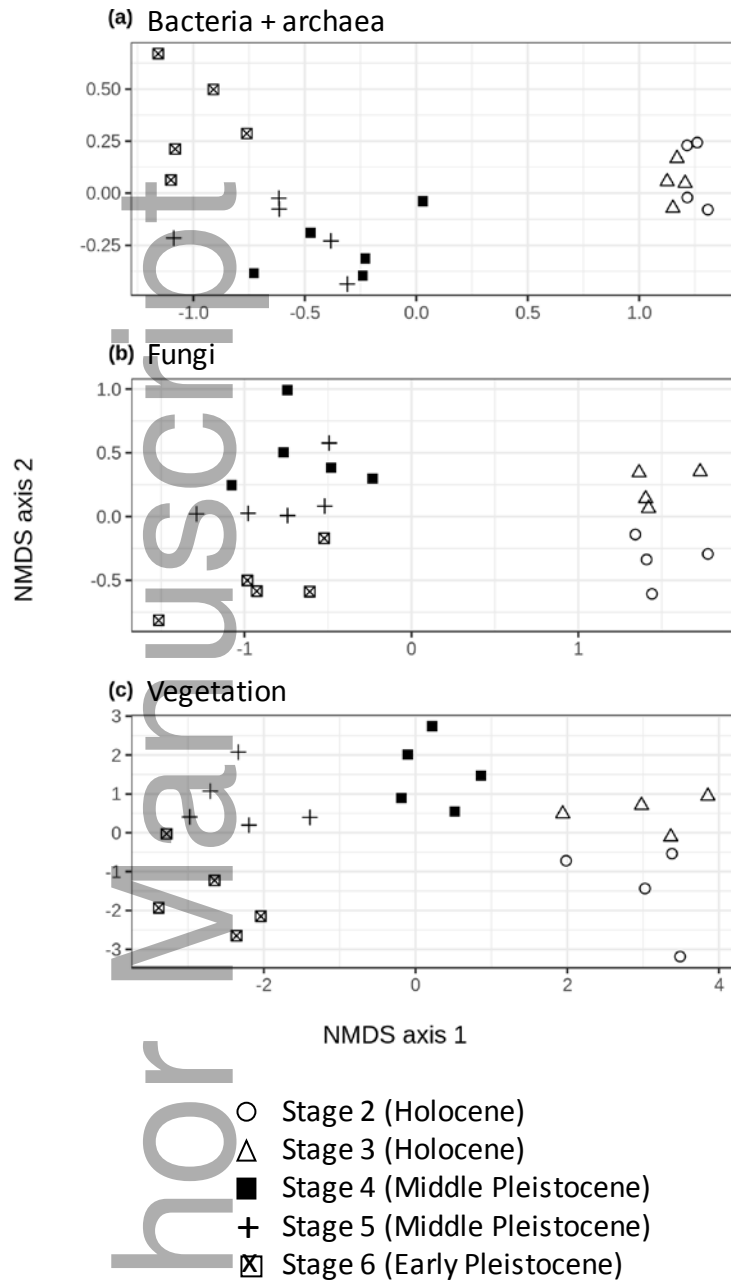


Figure 6. RDA ordination with Hellinger-transformed (a) 16S (bacteria and archaea) and (b) ITS (fungi) community data as the response to a combination of soil variables and nutrient acquisition strategies. Red lines are individual taxa (names omitted for clarity).

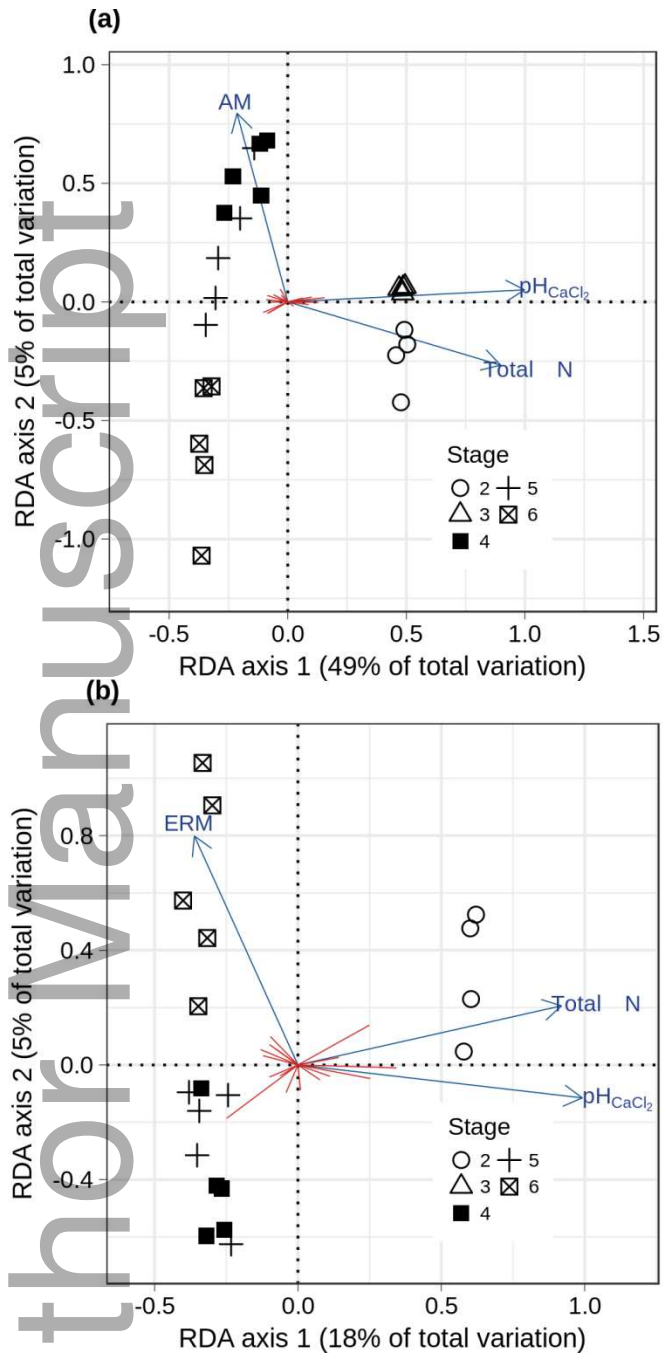


Figure 7. Means and 95% confidence intervals of the Procrustean association metric (PAM; procrustes residuals) against chronosequence stage from (a) the vegetation and ITS community data, (b) the fungal and bacterial community data, and (c) the vegetation and 16S data. In (a) and (b) the procrustes residuals are significantly greater on older soils, indicating increasing decoupling of the communities during long-term ecosystem development.

